AIAA JOURNAL
Vol. 49, No. 4, April 2011

Silent Owl Flight: Bird Flyover Noise Measurements

Ennes Sarradj,* Christoph Fritzsche,† and Thomas Geyer†
Brandenburg University of Technology, 03046 Cottbus, Germany

DOI: 10.2514/1.J050703

Most genera of owls (*Strigiformes*) have the ability to fly silently. The mechanisms of the silent flight of the owl have been the subject of scientific interest for many decades. The results from studies in the past are discussed in detail in this paper and the rationale for the present research is given, which included flyover noise measurements on different species of birds. Successful acoustic measurements were made on a Common Kestrel, a Harris Hawk, and a Barn Owl. Measurements on three other birds did not lead to reliable results. The setup and procedure used for the outdoor measurements are discussed. These include the estimation of the trajectory from dual video camera recordings and microphone-array measurements with a moving-focus beamforming technique. The main result from the 50 successful flyovers is that the owl flight produces aerodynamic noise that is indeed a few decibels below that of other birds, even if flying at the same speed. This noise reduction is significant at frequencies above 1.6 kHz. At frequencies above 6.3 kHz the noise from the owl remains too quiet to be measured.

I. Introduction

THE flight of most owl species is not audible to man and, more important, to their prey. This ability to fly silently has long been a source of inspiration for finding solutions for quieter flight and for noise reduction in fluid machinery. After more than a century the research regarding the mechanisms that enable the nearly silent flight of owls remains an interesting field for theoretical and experimental research. Many of these mechanisms have already been tested for their applicability in technical airfoils, resulting for example in sawtooth [1] or serrated trailing edges [2], comblike or brushlike flow-permeable trailing edges [3,4], or porous airfoils [5,6]. However, there are still a number of open questions.

One of these questions addresses the importance of each of the several adaptations of owls for quiet flight. How large is the potential noise reduction due to special morphological features? What is more important: the owl's ability to fly very slowly or the direct influence of the plumage morphology on the physical mechanisms of sound generation?

Several studies exist on the quiet flight of owls and on the special adaptations of their wings and feathers. To illustrate the motivation for recent bird flyover measurements subject to this paper, the following section gives a short overview on past research on the quiet flight of owls.

As early as 1904, Mascha [7] considered the morphology of bird feathers and noticed some special adaptations in owls that he made responsible for their quiet flight. This includes the comblike structure at the first primary feather of the owl wings, caused by the upward-bending of the barbs, and the long distal barbules (or hook radiates) of the owl feathers. These barbules end in the so-called pennulum, which is bent to the dorsal side of the feather. The first report on the silent flight of owls and a description of the special adaptations of the owl feathers responsible for the quiet flight was given by Graham [8] in 1934. He compared the wings and feathers of silently flying owls with the wings and feathers of an owl that belongs to a genus that does not fly silently, the Tawny Fish–Owl (*Ketupa flavipes*). Based on this comparison he identified three peculiarities of the owl feathers that are held responsible for the quiet flight: the leading-edge comb, the trailing-edge fringe, and the downy upper surface of the feathers. The photographs in Fig. 1 illustrate two of these adaptations: the leading-edge comb at the first primary feather of a Barn Owl (*Tyto alba*) wing and the trailing-edge fringe of the same wing. Graham also discussed the possible use of the silencing feather adaptations for aircraft and took into account the characteristics of the owl flight compared with nonsilently flying birds of prey: namely, the low wing loading and the low flight speed of the owl. Another detailed examination of the structure of the feathers of owls and other birds was done by Sick [9]. In partial reference to the results of Mascha [7], Sick [9] stated that the long, soft, upward-bent pennula cause a reduction of the noise that is generated by the friction between overlapping feathers.

The first published results on acoustical measurements were presented by Thorpe and Griffin [10], who noticed the lack of ultrasonic noise components (relating to frequencies above 15 kHz) in the flight noise of five species of owls, compared with other birds during flapping flight. Hertel [11] gave a short overview on the special feather structures of the quietly flying owls, including detailed microscopy pictures of the barbules. A thorough study on the low flight noise of owls and its utilization for quiet aircraft was done by Kroeger et al. [12] and Gruschka et al. [13] and published in 1971. Since this work is the basis for several other studies on the quiet flight of owls and contains results of acoustic experiments, it will be discussed here in more detail.

Kroeger et al. [12] performed acoustic flyover measurements on one specimen of the Florida Barred Owl (*Strix varia alleni*) in a 240 m^3 reverberation chamber. The room had reverberation times between 0.8 and 0.4 s for frequencies in the range of 100 to 10 kHz. The flight noise of the owl was measured using a single condenser microphone positioned slightly above the floor, with a distance to the flight path that was above the reverberation radius. The study focused on the noise generation during the gliding-flight phase only. This was judged by an observer who manually triggered the measurement. The data were recorded on magnetic tape. Later analysis produced third-octave-band sound pressure levels. The resulting spectra were then corrected for the background noise in the reverberation chamber.

The positions of the owl during flight (and, subsequently, its flight speed) were determined using a camera and two light flash units mounted to the ceiling of the room. The flash units were manually triggered by the observer, the first flash and photograph were triggered at the beginning of the gliding phase, the second at the end of it. The position was determined from the shadows cast on the floor and on the wall, which were both equipped with a tape grid pattern. The time interval between the two flashes was determined by reading the position of a black line on a white turntable, revolving with

Presented as Paper 2010-3991 at the 16th AIAA/CEAS Aeroacoustics Conference, Stockholm, Sweden, 7–9 June 2010; received 3 June 2010; revision received 29 September 2010; accepted for publication 12 December 2010.

*Junior Professor, Aeroacoustics Group, Institute of Traffic Research, Siemens-Halske-Ring 14.

†Research Assistant, Aeroacoustics Group, Institute of Traffic Research, Siemens-Halske-Ring 14.

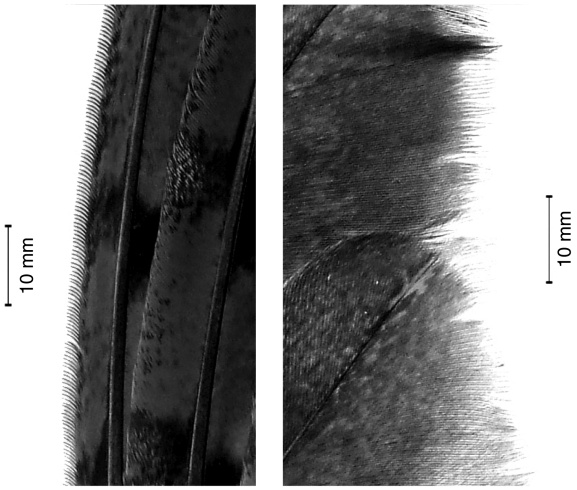

Fig. 1 Leading-edge comb (left) and trailing-edge fringes (right) of a Barn Owl.

constant speed, from the two respective photographs. It was attempted to keep the flight path of the owl constant by introducing a string barrier between an upper perch (starting position) in one corner of the room and a lower perch (landing position) in the opposite corner. Three test series were conducted. During the last test series, first the leading-edge comb and then a large portion of the trailing edge of the owl's wings were removed.

Figure 2 shows the third-octave-band spectra of four different flights labeled as good gliding phases. The original data presented by Kroeger et al. [12] are given as diffuse field sound pressure levels measured in a reverberant chamber. To enable comparison with flyover data from the present study, these values are transformed into free-field sound pressure levels by assuming equal sound power in the reverberant field and in the free field and an omnidirectional radiation pattern. The necessary values for reverberation time and volume of the chamber were also taken from [12].

In general, Kroeger et al. [12] found the shape of the sound pressure level spectra to be different from the flight noise of a sailplane, with a significant part of the noise energy being shifted to the low-frequency range of the spectrum below the hearing range of humans and the typical prey of the owls (mice and other small animals). Since the calculated total sound power of the gliding-flight noise was not low enough to be the only reason, the perceived quietness of the owl flight was found to be caused by this spectral shift. A dominant spectral peak was determined at approximately 15 Hz, which, unfortunately, matched the lowest fundamental mode of the reverberant chamber. No comparison of the measured flyover noise spectra of the Florida Barred Owl with other species was made

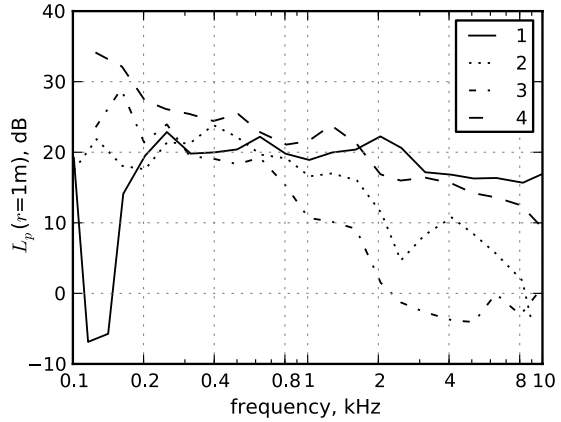

Fig. 2 Gliding flight noise of Florida Barred Owls (four individual flights, original reverberation room data from Kroeger et al. [12], transformed to third-octave-band free-field sound pressure levels L_p (re 2×10^{-5} Pa) in a distance of $r = 1$ m).

within the study. Although the sound power of aeroacoustic flight noise sources presumably has a strong dependence on the flight speed, no correction for different flight speeds was performed either.

Regarding the measurement setup, Kroeger et al. [12] described some general difficulties. For example, a large effort was required for the training of the owl to fly along the desired path in a reproducible way. Additional training was then required for the observer to trigger the acoustic measurement and the flash units at the correct time. As can be concluded from the number of flights and the reported flight quality, they also encountered complications from wing flaps during the gliding phase, with the wing of the owl touching the wall or other deviations from the correct flight path. In addition to these difficulties, another critical aspect of this study may be the small reverberation chamber in which the flyover measurements were made and the resulting predetermined short flight path of the owls that might not result in a natural flight behavior of the birds.

A comparison of the flight noise from Tawny Owls (*Strix aluco*) and Mallard ducks (*Anas platyrhynchos*) was presented by Neuhaus et al. [14]. Although the noise of the flying mallards was recorded outdoors, near a lake that the mallards frequently landed on, the measurements of the flight noise of the owls were conducted in a large gym on two tamed specimens, since their flight noise was too low to be measured in an outdoor environment. The outdoor flyover measurements on the mallards were done with a single microphone. The data were recorded on a magnetic tape recorder and analyzed using a B&K-type acoustic spectrograph. To reduce background noise, the measurements took place either early in the morning or late in the evening. The owls, however, had to fly from the hand of a trainer across a barrier with a height of 1.80 m to a landing spot at a distance of approximately 20 m, thereby flying over the microphone at a distance of approximately 0.3 to 0.5 m.

To analyze the influence of the leading-edge comb, additional acoustic measurements were done with the comb removed. No information is given on a measurement of the flight speed. According to Neuhaus et al. [14], the flight speed of a Tawny Owl is about 25 to 30 km/h (6.9 to 8.3 m/s) and that of the Mallard duck is about 60 to 75 km/h (16.6 to 20.8 m/s). However, the measured flight noise was not corrected for the different flight speeds of owls and mallards. The acoustic results are presented in a somewhat uncommon manner, with the amplitude of the noise signal given in scale divisions of the spectrograph, corresponding to the measured sound pressure, as a function of the (linear) frequency. The spectra are only shown for frequencies in the range of approximately 100 to 1.3 kHz, and a reference value for the chosen scale is not explicitly given. Instead, Neuhaus et al. specify an absolute sound pressure for the spectral maximum, enabling an indirect mapping of the scale divisions to sound pressure values. Further, the spectra are not given in conventional frequency bands, but using bands of 6% relative width, and the measurement distance is given as approximately 0.3 to 0.5 m. Using all this information, third-octave-band sound pressure levels for flyover in a distance of 1 m can be assessed to compare with other results. Figure 3 shows such sound pressure levels for a flight of the Tawny Owl with intact leading-edge combs and a flight of the owl with its leading-edge comb removed. From the differences in the flight noise spectra (in scale divisions) between owl and mallard and between owl with intact leading-edge comb and with leading-edge comb removed, Neuhaus et al. calculated differences of the sound intensity. This calculation includes the elimination of the background noise and is based on the sound propagation in the free field and an estimated distance between bird and microphone. For the gliding flight they found that the noise generated by the Mallard duck is in the range of 3 to 5 kHz, with its maximum around 4 kHz, and for the Tawny Owl the flight noise has a noticeable low-frequency character and ranges from 50 to 1.5 kHz, with its maximum at around 200 to 700 Hz. Based on Neuhaus et al., the ratio of the sound power generated by the Mallard duck to the noise generated by the Tawny Owl is about 30, based on the maximum amplitude of the flight noise only, and about 200 when referred to the whole frequency range. As was also stated by Kroeger et al. [12], Neuhaus et al. [14] drew the conclusion that the predominantly-low-frequency gliding-flight noise of the Tawny Owl cannot be heard by its prey, because their

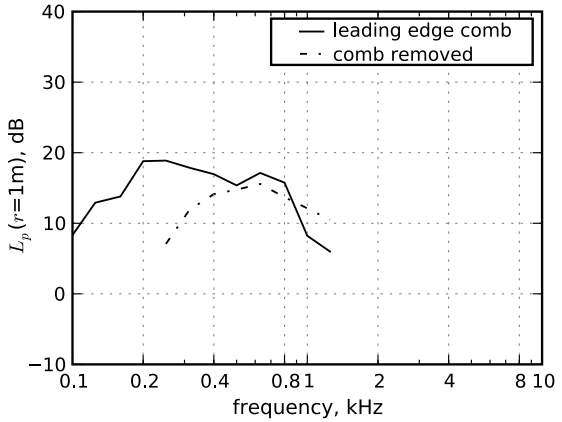

Fig. 3 Flight noise of a Tawny Owl during the gliding phase (original data from Neuhaus et al. [14], given in arbitrary scale divisions corresponding to the measured sound pressure in 0.3 to 0.5 m distance in frequency bands of 6% width, transformed to third-octave-band free-field sound pressure levels in 1 m distance).

hearing is very insensitive at low and medium frequencies. This is further illustrated by giving hearing threshold levels for some of the owl's typical prey (a locust, a moth, a rat, and a bullfinch), which are at least above 20 dB sound pressure level at 1 kHz and even higher for lower frequencies. The study by Neuhaus et al. gives a first proof that the flight noise of owls is indeed lower than that of other birds; however, it suffers from the differences of the measurement setup for mallard and owl, the acoustic measurement techniques available at that time, the differences of flight speed and weight of the birds, and the unusual presentation of the acoustic results.

More recently published analyses of the silent owl flight were done by Lilley [15,16]. Based on the work of Graham [8] and on data from Kroeger et al. [12], Lilley [15,16] concluded that the special feather adaptations of the owl lead to a major noise reduction above 2 kHz. He developed a simple model to estimate the flight noise of birds and technical gliders with masses between 1 and 400,000 kg, based on their mass and flight speed only. However, Lilley did not present any measured data and referred only to the flyover measurements by Kroeger et al. [12].

A detailed morphometric characterization of the wing feathers of a silently flying species, the Barn Owl, compared with that of a nonsilently flying species, the pigeon (*Columba livia*), was conducted by Bachmann et al. [17]. They provided a quantitative database of the feather structures of the Barn Owl and pigeon and of the special feather adaptations enabling the quiet flight of the owls. In a recent study, Geyer et al. [18] examined the noise generation of prepared wings of a Sparrowhawk (*Accipiter nisus*) and a Tawny Owl. Acoustic and aerodynamic measurements were conducted in an open-jet wind tunnel, with the ability to directly compare the noise generation for both species at the same flight speed. The results showed that the noise generated at the wing of the Sparrowhawk exceeded the noise generated at the owl's wing in the whole range of frequencies. The overall sound pressure level calculated from third-octave bands between 800 and 16 kHz of the owl's wing was below the overall sound pressure level of the Sparrowhawk's wing for all tested flight speeds between approximately 7 and 20 m/s. The experiments indicate that the quiet flight of the owl compared with other birds is indeed a consequence of the special feather adaptations and not only of its lower flight speed. The critical aspect of this study is the use of prepared-wing specimens that are possibly shaped in a way that does not necessarily represent the wing shape of a bird when flying under natural conditions.

All of these studies on the quiet flight of the owls show that the special adaptations of their feathers lead to a noticeable reduction of the noise that is generated during flight. But the very low sound pressure levels make it very hard to conduct acoustic measurements of the noise emission during the gliding-flight phase. And although measurements in an acoustic wind-tunnel are feasible and deliver comparable results, they do not take into account the natural flying condition of a bird flying outdoors. Past acoustic flyover measurements on owls were done indoors in order to avoid the dominance of background noise. Additionally, the reported measurements included the use of a single microphone only. The two most known acoustic experimental studies on the quiet owl flight, the work by Kroeger et al. [12] and Neuhaus et al. [14], show limitations regarding the measurement setup and leave a number of unanswered questions. In general, the acoustic measurements of the gliding-flight noise of owls in both studies were performed indoors in a reverberant environment, where the birds did not necessarily fly according to their natural habit. And whereas Kroeger et al. [12] did not measure the flight noise of a nonquietly flying bird at all, Neuhaus et al. [14] measured the flight noise of mallards, which have a much higher weight and fly much faster than the tawny owls.

This short summary of existing acoustic measurements of the flight noise of owls shows that further experiments, using up-to-date acoustic measurement techniques and techniques for the tracking of flight path and flight speed and taking into account the natural flying conditions of the birds, are reasonable and desirable. In the present paper, the realization and the results of acoustic flyover measurements on different species of birds, including owls and nonquietly flying birds of prey, are described. The experiments were performed using a 92-channel microphone array in an outdoor environment. The original motivation is a better understanding of quiet flight mechanisms and the transfer of knowledge to technical applications. Thus, similar to the studies in the past, the focus was on gliding flight, which seems to be more comparable with present technical devices.

The remaining part of the paper is organized as follows: First, the steps required to prepare and to perform the experiments are summarized, including a description of the birds and the experimental setup for the acoustic measurements and the measurement of the trajectory. Then details of the analysis are discussed: the estimation of the flight path and the flight speed of the gliding birds, as well as the processing of the acoustic data using beamforming algorithms in the time domain, are explained. Finally, results are presented and discussed.

II. Materials and Methods

A. Birds

As the research should deliver results regarding the flight noise from owls compared with other species, it was necessary to also include nonsilently flying birds in the analysis. The only option for having several different species available for testing was to use birds held in captivity. To perform the measurements, the birds have to cooperate and must be trained to do so. Although an indoor measurement setup can provide a quiet environment, considerable training of the animals is required. Thus, it was decided that the experiments should take place in an outdoor environment. Additionally, it is more likely in this case that the birds are flying according to their natural habit and under natural flying conditions. The main problem that arises from the outdoor measurement is that environmental conditions, such as rain (making measurements utterly impossible) or wind, have to be taken into account in the planning of the measurements and the presence of disturbing noise from other sound sources cannot be totally prevented.

The measurements were conducted in the wildlife park Johannismühle near Berlin on six different birds, belonging to three nonquietly flying species (Common Kestrel, Harris Hawk, and Saker Falcon) and two quietly flying species (Barn Owl and Eurasian Eagle Owl). Table 1 gives an overview of the birds. The animals belonged to a falconry that is part of the wildlife park and presents the birds in two public shows per day. The measurements had to be conducted in the break between the two shows, leaving a time frame of 3 h to install the equipment, perform the tests, and unmount the equipment. Since each bird would only do a certain number of flights per day, is was not possible to include all birds in a single measurement campaign. Instead, only one or two birds were taken out of the public program and were available for the measurements per day. Not all birds that are shown in the public shows could also be used for the test. The

Table 1 Birds used for the test

Species	Genus	Mass, g	Wingspan, cm (approx.)
Common Kestrel (*Falco tinnunculus*)		198	59
Harris Hawk (*Parabuteo unicinctus*)		660	95
Saker Falcon (*Falco cherrug*)		940	100
Barn Owl (*Tyto alba*)		298	84
Eurasian Eagle Owl (*Bubo bubo*), male		1630	120
Eurasian Eagle Owl (*Bubo bubo*), female		2420	133

eagle, for instance, might have destroyed the measurement equipment in an attempt to explore it.

For the experiments, the birds were mostly flying from the hand of one falconer to a second falconer, who lured the bird with food. One of the Eagle Owls flew from one perch to another and the Saker Falcon was flying in circles diving for a bait fixed on a flexible pole and operated by one falconer. The advantage of the respective methods was that the birds were already trained to do the exact same procedure for the public shows of the falconry, and hence no additional training of the birds was necessary. The falconers were instructed to try to influence the flight trajectory of the birds by changing their distance and the position and posture of their hand in a way that the bird was flying in gliding flight above the microphone array (without flapping of the wings). Each flyover ended with the bird decelerating its flight by stalling its wings and moving steeply upward to land on the hand of the falconer. This flight phase was excluded from the analysis. Figure 4 shows a photograph of a flyover measurement on a Barn Owl, which is just flying over the camouflaged microphone array toward one of the falconers.

Circumstances that noticeably complicated the measurements and the postprocessing of the data were the background noises, caused either by rustling leaves on nearby trees, ambient sounds from distant sources, or the other birds of the falconry, which were occasionally shrieking.

B. Measurement Setup

The setup for the acoustic measurements had to meet a number of requirements. First, since it had to be used outdoors on a grassland area, its construction had to be sufficiently robust and insensitive to moisture. Second, the short time frame between the two public shows of the falconry required a setup that could be assembled and disassembled very fast, with very little adjustments required. Finally, in order to not distract the bird from its daily routine, it was necessary to camouflage parts of the equipment using green-colored cloths made of lightweight fabric that was highly permeable to air and to sound.

The low gliding-flight noise of owls required an acoustic measurement setup that is very sensitive and allows for the efficient suppression of background noise to provide a signal-to-noise ratio that is as high as possible. Additionally, it should provide a sufficient spatial resolution to localize the sound sources connected with the flying birds. The acoustic measurements were conducted using a 92-channel horizontal microphone array mounted on the ground. The array consisted of a planar 0.5×0.5 m center array that holds 64 flush-mounted $\frac{1}{4}$ in. electret microphone capsules and four linear extensions, each holding additional seven $\frac{1}{4}$ in. microphones with logarithmically scaled spacing. The four extensions were mounted to the sides of the center array, increasing the aperture of the complete array to 3.5 m (see Sec. II.D for further details). The microphones were connected to a computer-controlled front end and were sampled using a frequency of 61,440 Hz and a respective alias-free bandwidth of 29,800 Hz. The resulting data were recorded and processed at a later time.

Another aspect of the flyover measurement setup that had to be considered carefully was the measurement technique applied to capture the flight path and the speed of the bird. Although it is also necessary to know the trajectory of the object under test in vehicle drive-by or airplane flyover measurements using an array, the techniques implemented (see, e.g., Guérin et al. [19]) in such cases could not readily be applied here. For example, it is not possible to use Global Positioning System, light barriers, laser distance meters, or any sort of markers to track the flying birds. Application of such devices would possibly harm the animals, could cause distress, and would violate the Animal Welfare Act. In addition to that, the method had to allow deviations from the desired flight path above the array up to a certain degree, which is difficult when using light barriers. Thus, two charge-coupled-device (CCD) video cameras (The Imaging Source, type DMK 21BG04.H, Gigabit Ethernet CCD monochrome camera, 640×480 pixels) were used to capture the flight path. The camera signals were transmitted via Gigabit Ethernet to the same computer that was recording the microphone signals and recorded synchronously with these signals. The frame rate was set to 30 frames/second, thus resulting in 2048 audio samples per video frame.

The cameras were positioned at a height of 1 m above the array center, with the camera axes perpendicular to each other and parallel to the ground, meeting at a point 1 m above the array center. The distance of the cameras from this point was 10 m, and the distance between the cameras was 14.14 m. Figure 5 shows a scheme of the

Fig. 4 Barn Owl (*Tyto alba*) flying over the camouflaged microphone array toward one of the falconers.

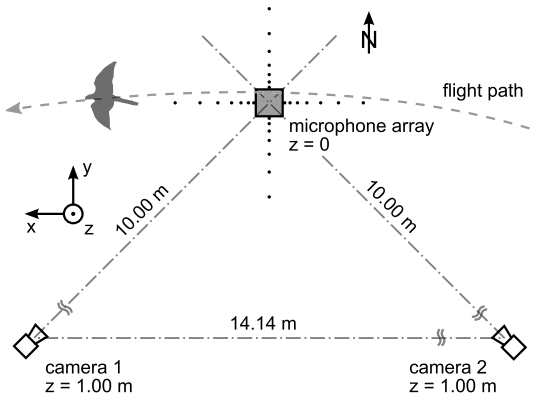

Fig. 5 Schematic top view of the measurement setup used for the bird flyover measurements.

measurement setup, including the microphone array, consisting of a square center array and four linear extensions, the two CCD cameras, and a possible bird flight path.

The general procedure of the flyover measurements was as follows: When the bird started its flight, an observer triggered the synchronous recording of both the microphone array and the camera signals. When the bird had passed the microphone array, the observer triggered the end of the recordings. Any necessary labeling of the measured data was done completely during the postprocessing of the data. Therefore, it was also possible to capture more than one flight during one active measurement.

Measurements were only performed under dry weather conditions (no rain or fog) and with wind speeds below 3 m/s. To monitor this, a portable weather station (type PCE-FWS 20) was used that recorded the wind speed with an relative accuracy of 10% and the temperature with 0.1°C accuracy. The recorded wind speed was also used together with the wind direction to correct the bird speed over ground to airspeed during the subsequent analysis. The temperature was used to estimate the correct speed of sound to be used in microphone-array data processing.

C. Flight Trajectory

The videos recorded by the two cameras were processed to get an estimate of the flight trajectory of the birds. The basic idea of the technique applied was to track the position of the birds in the videos from frame to frame and then to combine the results from both cameras to find the position over time in three dimensions.

A number of different image processing techniques are available to track objects within a video sequence [20]. These techniques generally rely on the determination of the apparent motion of optical features within the recorded scene. The pattern of this apparent motion is called optical flow and consists of one velocity vector per pixel for each frame of the video sequence. The calculation of optical flow is possible by different methods. Some of these methods, such as the Lucas–Kanade method [21], need optical features like shape outlines that have to be identified in the image before application. Since the birds are constantly changing their apparent shape during flight, these techniques turned out to be not applicable in the present case. Instead, the Horn–Schunck [22] method that not only processes local regions, but also the whole image (dense optical flow), was chosen.

Because the cameras have fixed positions in the setup, it is reasonable to assume that the background image changes very little, leading to low or zero values for the optical flow at all pixels that belong to the background. In contrast to this, a fast-moving bird leads to high values of the optical flow at those pixels in the image that show the bird. Then the location of the maximum amplitude of optical flow should identify the bird. However, this maximum does not mark some fixed point on the body of the bird, but only some arbitrary part of it that moves fastest at the respective instant. This could be, for example, the wing tip or the tail. As this part of the body may change from frame to frame, it cannot be readily assumed that the maximum moves exactly at the same speed as the bird. If the sequence of maximums is taken as a representation of the track, this introduces a considerable random error.

Another complication arises from other moving objects in the video, such as persons (the falconers) and other birds passing the scene in a greater distance. In some of the frames the location of the maximum amplitude of optical flow may correspond to these objects. If a sequence of maximum locations (one for each frame of the video) is calculated, most of them can be expected to be somewhere on the bird, but some others may be at completely different parts of the video image. The latter need to be removed to obtain a discontinuous representation of the track from the remaining sequence.

An improved estimation of the flight trajectory with reduced random error from the sequence of locations of maximums requires the application of a model for the trajectory, such as the assumption of a certain direction or speed. Bird flight is typically not straight and does not have a constant speed. Thus, for the present research, a more flexible model for the trajectory was applied. It was assumed that both the change in direction and the change in speed were small between individual video frames. This model was implemented by not taking into account any maximums found that resulted in abrupt changes of direction or speed of the tracked object. Thus, other objects (such as persons or other birds) connected with maximum amplitudes of optical flow in some frames had no adverse effect. The result from this tracking process was a sequence of image coordinates u_i and v_i over time. To remove the noise in this estimate, a fifth-order polynomial fit turned out to be sufficient. Thus, the final results from the tracking were smooth functions $u_1(t)$ and $v_1(t)$ for camera 1 and, similarly, $u_2(t)$ and $v_2(t)$ for camera 2.

From the image coordinates of camera 1 and the unknown camera-object distance r_1, an estimate $\mathbf{X}_1$ for the three-dimensional coordinates of the object may be calculated. Likewise, a similar estimate $\mathbf{X}_2$ may also be calculated from the image coordinates of camera 2 and the respective camera-object distance r_2. The unknown r_1 and r_2 can then be found from an iterative minimization of the distance $\|\mathbf{X}_1(r_1) - \mathbf{X}_2(r_2)\|$ between the estimates. Tests with artificially marked objects placed above the microphone array in the region of interest for tracking the flight trajectory showed that this procedure gives an estimate of the position with less than 10 cm error in all three coordinate directions.

This procedure was repeated for every time step t_i, and the trajectory, given as $\mathbf{X}(t_i) = (\mathbf{X}_1 + \mathbf{X}_2)/2$, was calculated. Thus, the position of the bird at every $1/30$ s was known. The position for any t between the t_i was calculated using spline interpolation. This technique resulted in the possibility to estimate the position of the bird at any instant during the flight over the setup. An example for a flight trajectory calculated by application of this method is shown in Fig. 6. The flight was a gliding flight in the positive x direction. It can clearly be seen that in this case the bird flew on a trajectory that was bent upward.

For the analysis of the noise generated during flight, it is also important to know the flight speed. This information is readily available from the trajectory. As the speed was not constant, an average over a certain length of the trajectory was calculated that corresponds to the same segment of the trajectory that was considered in the acoustic measurements.

D. Microphone-Array Beamforming

1. Theory

The beamforming algorithm that was used is based on the assumption that a source is moving in front of an array of microphones on an arbitrary trajectory with variable speed. The signal $s(t)$ emitted by this source at a certain time t at its current position $\mathbf{X}_s(t)$ travels a distance $r_{m,i}(t) = (\|\mathbf{X}_s(t) - \mathbf{X}_i\|)^{\frac{1}{2}}$ to the microphone i at $\mathbf{X}_i$ that is part of the array. If the air is at rest, the sound pressure at the microphone due to the source is

$$p_i(t + \Delta t_i(t)) = s(t)/r_{m,i}(t) \tag{1}$$

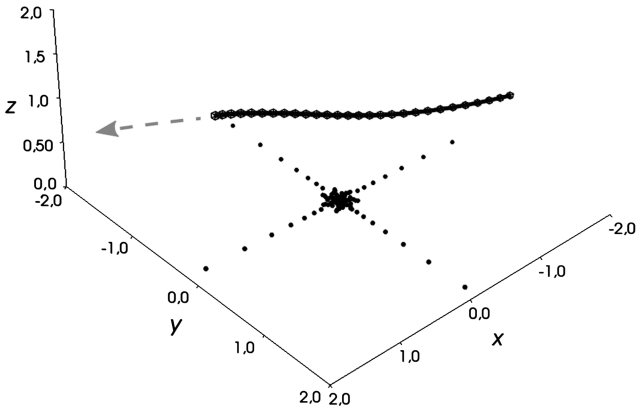

Fig. 6 Example for a flight trajectory (thick line) captured from the two video sequences (the black dots show the microphone positions and the arrow indicates the direction of flight).

where the time delay is given by $\Delta t_i(t) = c/r_{m,i}(t)$ with the speed of sound c. Both the source-microphone distance and the delay are functions of time due to the motion of the source.

The basic idea of beamforming is to focus on an assumed source position and to apply a signal processing to the microphone signals such that an output is generated that meets two important conditions. First, if the assumed source position is the actual position of the source the output should be the source signal itself, possibly scaled by some known factor. Second, if the source is at any other location, the output should be minimal and in any case its amplitude less than that of the source signal. With these properties the beamformer is a directional sound receiver with true three-dimensional directivity characteristic. The typical application is to steer the beamformer consecutively to several assumed source positions with a regular grid. From the outputs, a map of sound sources (beamforming map) is constructed.

The first condition for the beamformer map is easily fulfilled. The signal processing only needs to inversely apply the relation from Eq. (1) and thus compensate for the delay and attenuation of the signal. The output of the beamformer for an N-channel microphone array can then be calculated from

$$p_o(t) = \sum_{i=1}^{N} h_i p_i(t + \Delta t_i(t)) \tag{2}$$

where h_i are the steering factors. One possible choice for these factors would be $h_i = r_{m,1}/N$. This would result in $p_o(t) = s(t)$, if the source is at the assumed position and thus would meet the first condition. However, the second condition is not necessarily met. If the actual source is in the same direction as the assumed source, but at a somewhat closer distance to the array, the beamformer output may be larger than the source signal.

To also meet the second condition, a more sophisticated approach is required. The choice of

$$h_i = 1 \Big/ r_{m,j} \sum_{j=1}^{N} r_{m,j}^{-2} \tag{3}$$

also meets the first condition. At the same time it can be shown [23] that it minimizes the output power of the beamformer in the case of a large number of noncorrelated sources that are randomly distributed in space. Such a configuration would produce spatially white noise with a covariance between the microphone channels that vanishes, except for $i = j$. If the beamformer output power is minimal under such circumstances, it can also be concluded that the second condition is fulfilled.

The source signal s as defined in Eq. (1) can be interpreted as the sound pressure a monopole source would produce in a certain distance r_0 multiplied by that distance. If the beamformer output is multiplied by that distance, it can be readily taken as the sound pressure of the source in the distance r_0. A common choice for r_0 is the distance between assumed source and array center [24].

A typical beamforming map shows the mean square of the beamformer output or the sound pressure level calculated from it. A commonly applied method to produce better looking images is to remove the autocorrelation terms within the averaging process using

$$p_{rms}^2(t) = \left\langle \left(\sum_{i=1}^{N} h_i p_i(t + \Delta t_i(t)) \right)^2 - \sum_{i=1}^{N} (h_i p_i(t + \Delta t_i(t)))^2 \right\rangle_T \tag{4}$$

where $\langle\,\rangle_T$ denotes the time average. This is equivalent to the deletion of the main diagonal of the cross spectral matrix [25] that is used in the frequency-domain formulation of beamforming. The effect is the removal of the influence of noise that is uncorrelated between the individual microphone signals [26]. Such noise is mostly not of acoustic origin, but is generated by nonacoustic pressure fluctuations at the microphones and by the microphone electronics and data acquisition. However, if the beamformer is steered to regions where there is no source, this approach may lead to some negative values for $p_{rms}(t)^2$, which must be set to zero to remain physically correct.

In some cases it is an advantage to apply additional weight factors w_i to the individual channels. This can be done by using modified steering factors according to

$$h_i = \frac{w_i}{r_{m,j} \sum_{j=1}^{N} (w_j r_{m,j}^{-2})} \tag{5}$$

2. *Microphone Array*

The microphone layout of the array determines the properties of the beamformer. These properties can be measured using the beamforming map that is produced as the image of a single point source. This image, the point-spread function, shows a main lobe where the source is and side lobes of lower levels at other positions. The main-lobe width, which should ideally be very small, is determined by the quotient of wavelength and array aperture. Thus, for low frequencies and long wavelengths, a large array is needed. The dynamic range between the main lobe and the side-lobe levels is controlled by the geometric arrangement [24] and the number of microphones and also depends on the frequency. Thus, there is no microphone layout that produces optimal beamformer properties for all frequencies. One possible solution is to use different layouts for different frequencies. A practicable implementation is to use different subarrays within one and the same array for different frequency ranges. An additional possibility is the use of weight factors that has an influence on both the main-lobe width and the side-lobe levels.

The microphone array (Fig. 7) used for the bird flyover measurements was designed to work in the frequency range from 500 Hz–10 kHz. In the central part of the array, 64 microphones were arranged in seven logarithmic spiral arms. This arrangement (Fig. 8) was numerically optimized for measurements above 6 kHz, but does not deliver a sufficient resolution for lower frequencies. The aperture of the array was enlarged to 3.5 m with four linear extensions, each equipped with seven logarithmically spaced microphones. This enlargement provided a sufficient resolution down to 800 Hz and down to 500 Hz when using weighting factors, such that the processed acoustic power per unit area was approximately constant, as proposed by Sijtsma and Stoker [27]. This approach essentially favors the signals from microphones from those parts of the array

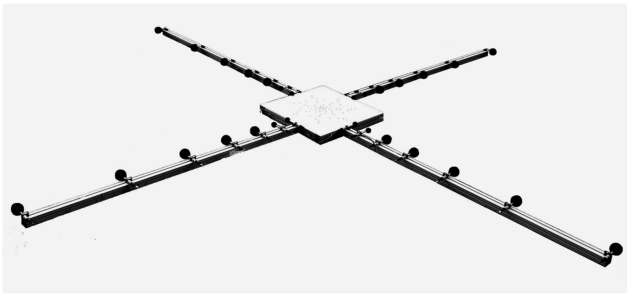

Fig. 7 Photograph of the microphone array.

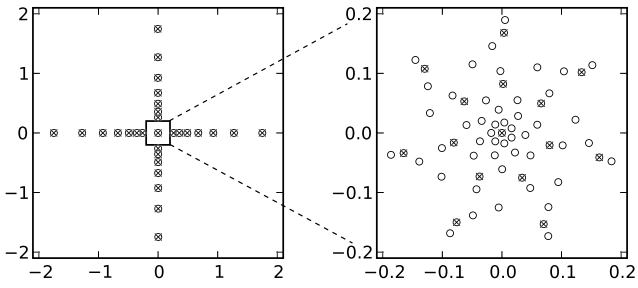

Fig. 8 Microphone layout with 29 microphones and the central part with 64 microphones (magnified). Those microphones that were part of the 43-microphone arrangement are marked with a cross.

with larger microphone spacing. Although a layout with a more uniform distribution would have delivered better properties, especially for lower frequencies, it could not be realized due to practical issues.

In consideration of the frequency-dependent properties, different subarray layouts were applied in the analysis. For the frequency bands 500 Hz–1.25 kHz, a 29-microphone layout was used that consisted of one center microphone and microphones at the four extensions. For the 500 and 630 Hz third-octave bands, weighting factors were applied. The 43-microphone layout for the bands 1.6–2.5 kHz used the microphones at the extensions and 15 selected microphones from the center array. All 92 microphones were used for 3.15–5 kHz, and only the center 64 microphones were used for the bands 6.3–10 kHz. Figure 9 shows examples of the point-spread function for each of the subarrays used. These point-spread functions were calculated for a fixed source in a distance of 0.9 m from the array center. For sources at other locations, the point-spread functions vary.

3. *Source Power Integration*

Although it is possible to identify sources within a beamforming map, the estimation of the source level is not straightforward. In the process of beamforming the true source image is convolved with the point-spread function. Thus, depending on the point-spread function, the map will show an enlarged source region. Integration over this region yields not the total source level, but a value that is greater, due to the main-lobe width. One possible solution is the deconvolution [28,29] of the map to get the true source image and correct source levels. However, in the case of moving sources, this is computationally very demanding.

Another technique that is applied in the present analysis is the source power integration technique [27]. In this approach, the estimated beamforming map of the source is compared with that of a single source, and the respective point-spread function is used to obtain the correct level. It is assumed that the source or sources of interest are within a certain sector of the map. Integration over this sector then gives a value P_1. To take the array characteristics into account, the point-spread function for a point source of known source power P_s in the center of this sector is calculated and integrated to give P'_1. Then $P = P_s P_1 / P'_1$ is taken as an estimate of the true source power.

This technique is applicable as long as the main lobe of the point-spread function is much smaller than the map sector used for integration. Sources mapped outside the sector may lead to wrong estimates if they produce strong side lobes within the sector. The influence from sources outside the sector can be minimized in both integrations if any parts of the map are neglected that are more than a certain level difference Z below the peak value found in the sector. In the present analysis it was found that the choice of Z (finally set to 6 dB) had only little influence (less than 1 dB) on the result, as long as the dynamic range of the map within the sector was larger than 4 dB. Thus, it can be concluded that the source power integration technique itself introduces a negligible error in the result.

4. *Implementation*

To process the data recorded during the flyover measurements, an in-house software was applied that uses a combination of the programming languages Python and C and routines from the SciPy library. Equation (4) was implemented using the steering factors from Eq. (5). The assumed source positions were arranged in a planar map grid. The required distances between the grid points and the microphones were calculated under the assumption that the map grid moves along the trajectory. Thus, these distances had to be recalculated for every sample that was processed. The microphone signals $p_i(t + \Delta t_i(t))$ that are used in Eq. (4) were linearly interpolated from the available samples.

To obtain spectra of the sound sources, the signals were filtered using third-octave-band digital filters. The straightforward application of these filters introduces a frequency-dependent phase delay that would distort the beamforming result. Thus, the filters were applied twice to the signals. In the first pass the signal was filtered as usual, and in the second pass the filtered signal was processed again, but with reversed time history. Thus, the filters had a zero phase delay [30], and no additional delays were introduced in the beamforming algorithm.

For each third-octave band a separate beamformer output was calculated using the appropriate microphone channels, microphone layout coordinates, and weighting factors. Finally, the beamformer output was linearly averaged over short time segments. From the results of this averaging, a sequence of beamforming maps was assembled. The maps in this sequence show the contributions to the sound pressure that would be measured in the array center for each of the respective segments of the trajectory. From these sequence maps an overall result map was calculated for each frequency band. Since the distance from the source to the array center varied considerably during one overflight, this map was computed as an average weighted according to the source power integration technique to remove the influence of this varying distance. Likewise, the overall source power was calculated for each frequency band, making use of the source power integration technique, where the integration was carried out over appropriate sectors in the maps.

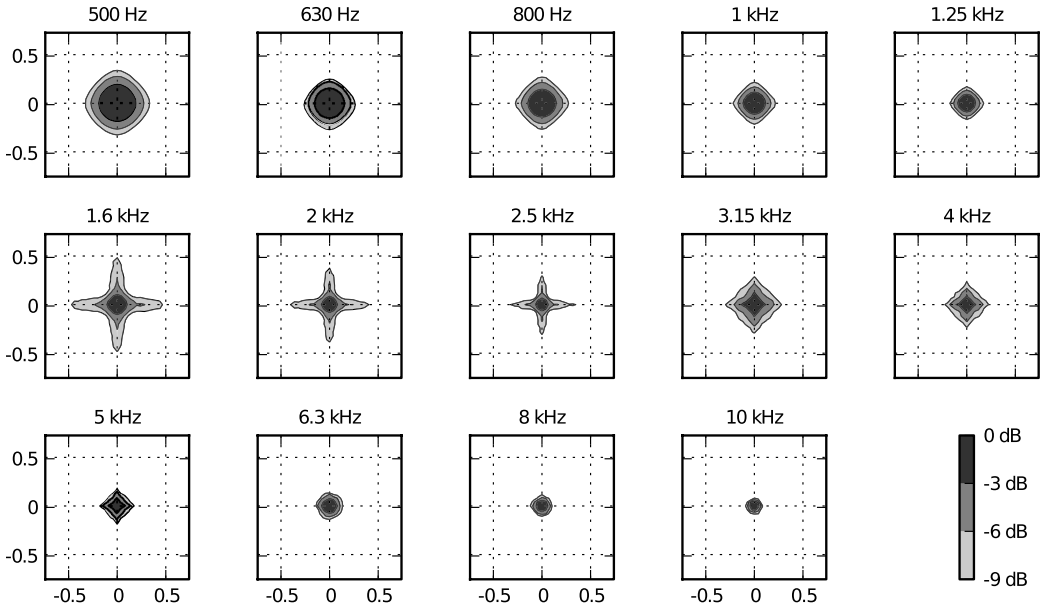

Fig. 9 Point-spread functions of the microphone array for a fixed source in a distance of 0.9 m from the array center. Coordinates are given in meters.

Table 2 Summary of flights analyzed for flight noise

Bird	No. of flights	Flight speed, ms^{-1} Mean	Std. dev.	Min	Max
Common Kestrel	31	5.2	0.54	3.8	6.2
Harris Hawk	5	5.3	0.76	4.2	6.4
Barn Owl	14	5.4	0.64	4.6	6.7

III. Results

During the measurement campaign, the flight performance varied greatly between the birds. The Common Kestrel showed the greatest endurance, flying for more than 20 min from one falconer over the microphone array to the other falconer, with more than 100 flyovers. Both the Harris Hawk and the Barn Owl did more than 25 flights. The Saker Falcon and the two Eagle Owls only did between 10 and 20 flights. The larger birds, especially, had to be rewarded with food after nearly every flight. When they had enough food for the day, they could not be motivated to perform further flights.

The focus in the present study is on gliding flight. Naturally, birds are not exclusively in a gliding phase during flight, but also show flapping flight and other maneuvers. Thus, the flights of interest were only those in which the birds were in a gliding phase when flying over the array. This was the case in about one-fourth of all flights. Two additional factors further reduced the number of flights available for noise measurements. First, the birds were occasionally shrieking during flight. These loud vocalizations were masking the flight noise entirely. Second, despite the efforts of the falconers, the larger birds often chose flight trajectories that went too far from the array for any measurement. In the end, for the Saker Falcon and the Eagle Owls, there remained no flights that could be successfully analyzed for the flight noise.

For the other species, Table 2 summarizes the flights and gives the flight speed relative to air. Interestingly, the mean flight speed was not very different for these three birds, whereas a somewhat greater variability could be observed for the flights of individual birds. The measured flight speeds match the natural flight-speed range for a Barn Owl. Both the Common Kestrel and the Harris Hawk could fly considerably faster. However, due to the short flight distance in the setup, it seems to be inefficient to fly at a higher speed and, consequently, the birds did not do so. Although this is a deviation from their natural behavior, the similar flight speeds did simplify the comparison with the owl flight.

The microphone array has the best spatial resolution for sources that are directly in front of the array. The viewing angle between the direction of the source as seen from the array center and the axis perpendicular to the array should not be too large. To keep this angle small, the array measurements were not analyzed for the whole flight, but only for a fraction of it. Only those parts of each flight trajectory were taken into account that were within a 0.6 m horizontal distance from the array center axis. As the minimum flight altitude was also 0.6 m, the angle was thus limited to 45°. However, this limitation resulted in very short time periods available for analysis. Depending on the trajectory path and the flight speed, these time periods varied approximately between only 50 and 250 ms for a single flight.

For each of the flights, maps of sound pressure contributions for the third-octave bands between 500 and 10 kHz were calculated. As past findings suggest the importance of low-frequency sound to owl flight noise, results for lower frequencies also would have been of interest. However, the resolution of the microphone array was not sufficient for frequencies below the 500 Hz third-octave band, rendering such results invalid. The maps give the sound pressure level that would be measured in a 1 m distance from the bird if the sound radiation has an omnidirectional polar pattern. Because of the small viewing angle, it is feasible to neglect the true polar pattern, as it would result in only very small differences along the part of the flight trajectory accounted for. This is true even if a strongly directional, dipolelike polar radiation pattern would be assumed.

The maps are computed in a coordinate system fixed at the flying bird. In Fig. 10 one example is shown for a flight of the Common Kestrel. There are no large differences between the frequency bands. Thus, the flight noise appears to be purely broadband, with no distinct tonal components. Because of the different array characteristics in the individual frequency bands, the maps show a frequency-dependent image of the position of the sound sources. However, for some frequency bands, two source regions can clearly be recognized. These source regions seem to correspond to the wings of the bird. Although the true position of the bird's wing edges and tips cannot be estimated with sufficient precision to draw a direct conclusion, it is reasonable to assume that the corresponding major sound sources are located at the wing trailing edge and possibly also at the wing tips. This would be the case if the wings were technical airfoils not permeable to flow, having a distinct trailing edge, and experiencing an inflow that is not very turbulent.

In addition to one or two main maximums, extra maximums of smaller amplitudes appear as "islands" in the maps. These are associated either with minor sources or with side lobes resulting from

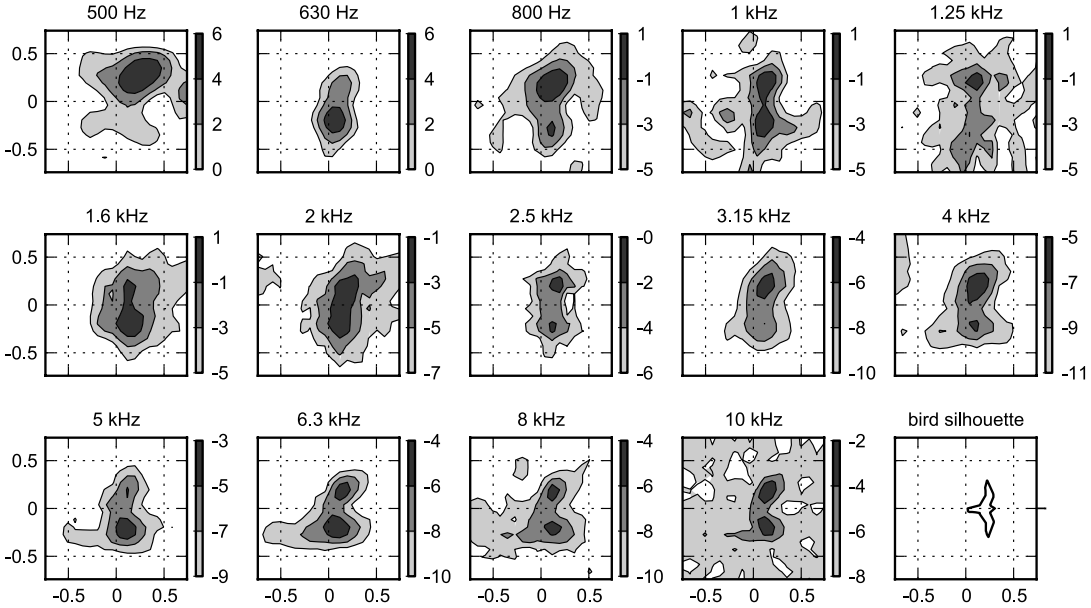

Fig. 10 Maps of third-octave-band sound pressure level contributions (in decibels) for a flight of the Common Kestrel. Coordinates are given in meters. The bird silhouette indicates the approximate location of the bird and the direction of flight.

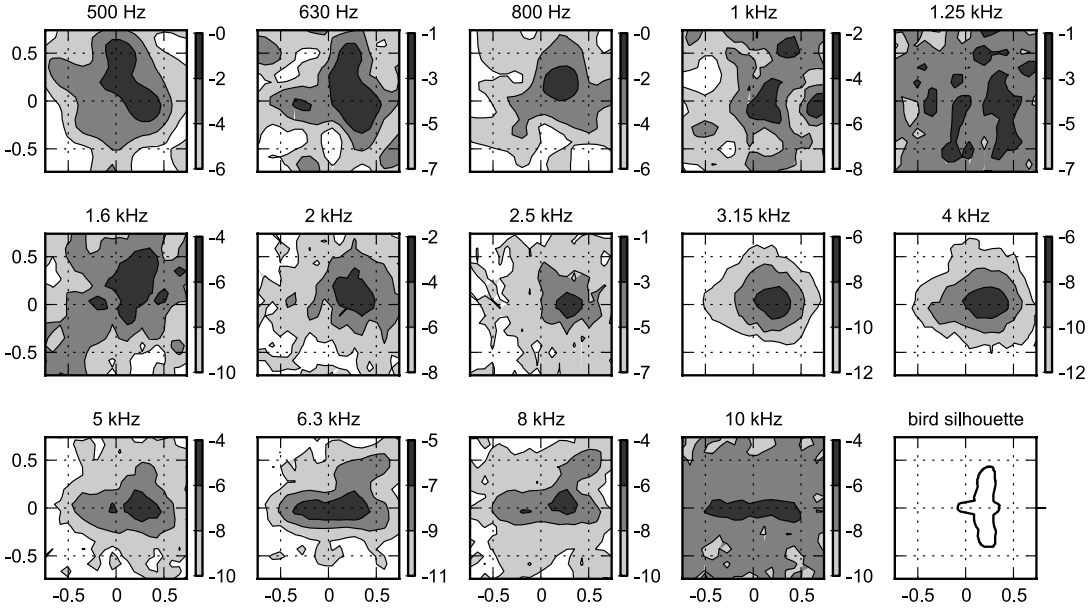

Fig. 11 Maps of third-octave-band sound pressure level contributions (in decibels) for a flight of the Barn Owl. Coordinates are given in meters. The bird silhouette indicates the approximate location of the bird and the direction of flight.

the convolution of the source distribution with the point-spread function that varies strongly along the trajectory. Although the error introduced by the latter was accounted for in the source power integration for the quantitative results, it was not possible in the present analysis to remove the side lobes from the maps as this would have required the application of a deconvolution method. The map for the 10 kHz band has a reduced dynamic range due to background noise that could not be removed by using the microphone array.

Although the results for the Harris Hawk are similar to those for the Common Kestrel, the results for the Barn Owl are different. Figure 11 shows example maps for a flight of the Barn Owl. Although the noise is also broadband, the level is smaller for most frequency bands and the source region is less distinct. Instead, even for those frequency bands with a high spatial resolution of the microphone array, there is only one larger source area. It is not possible to identify distinct sources as in the case of the Common Kestrel and the hypothesis of the major sound source being the wing trailing edge and wing tips does not hold. Instead, the sound emitted during flight presumably originates from a number of sources of approximately equal power distributed on the surface of the body, the wing, and possibly feet and legs. Therefore, it may be concluded that the mechanisms of the sound generation are different in owl flight and the fringes and possibly other adaptations found in the owl prevent the wing trailing edges from being major sources.

Some of the maps in Fig. 11 also have a very limited dynamic range. This indicates that the sound to measure is indeed very weak and at the lower limit of what can be measured at all with the setup. This could also be confirmed when analyzing the recordings from an arbitrary array microphone. In this case, no significant difference was found between the third-octave-band spectra during a flyover and without a bird present over the array. Additionally, the owl flyover was not audible at all when listening to a single microphone recording, whereas for the Common Kestrel a very faint swishing could be detected within the background noise.

Third-octave-band spectra were calculated from the maps of sound pressure contributions for all flights using the source power integration technique. The integration was performed over a sector of 1.2 by 1.2 m centered at the bird. Any map with a dynamic range less than 4 dB in this sector was not considered in order to limit the influence of background noise on the results. The results for the sound pressure level L_p in a distance of 1 m from the source were averaged for each of the three species to produce the result shown in Fig. 12. In the two highest frequency bands, no reliable results could be calculated for the Barn Owl due to the low dynamic range of the respective maps. For the other frequency bands, the majority of the maps could be included in the calculation.

The spectra show that the Barn Owl has a lower flight noise than both the Common Kestrel and the Harris Hawk for frequency bands of 1.6 kHz and above. The difference is only a few decibels. However, it appears to be significant when the standard deviation of the results, as indicated in Fig. 12, is taken into account. As the flight speeds of the birds were not too different, an important conclusion can be drawn: The silent flight of the owl is not only a consequence of its low speed. Instead, a mechanism or device found only in the owl makes it fly more silently. Very likely, the adaptations of the owl's feathers, as mentioned by Graham [8], are to be held responsible for this difference.

A more in-depth comparison of the results needs to account for the different speeds of the individual flights. Any scaling with respect to flight speed requires a hypothesis regarding the speed dependence of the sound power. If trailing-edge noise is the predominant noise source, dependence on the fifth power of the speed [31] can be assumed. The same assumption is made in Lilley's [15] generic formula for clean airframe and bird noise. However, this assumption is not valid if the trailing-edge noise is not predominant, as found for the owl from the maps in Fig. 11. Although, in theory, the scaling law appropriate for the owl could be estimated from the measurements itself, this was not possible because of the limited variability of the

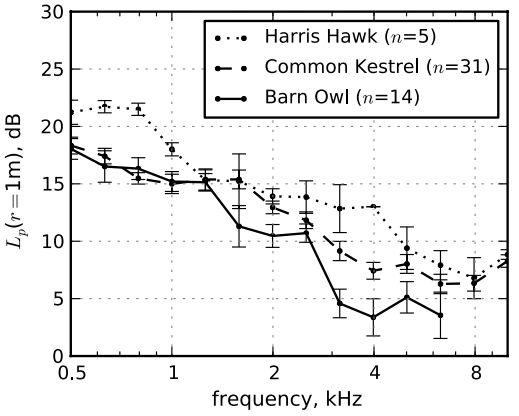

Fig. 12 Third-octave-band spectra from the flyovers, mean values, and standard deviations for *n* flights per bird (see Table 2).

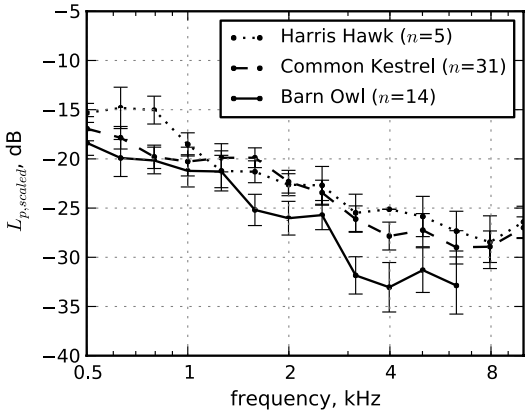

Fig. 13 Scaled third-octave-band spectra from the flyovers, mean values, and standard deviations for *n* flights per bird (see Table 2).

flight speed. The analysis of prepared specimen in the wind tunnel done in a different study [18] also did not lead to definite results for a scaling law. Thus, in the absence of a better hypothesis, all results (including those from the owl flights) were scaled with the fifth power of the flight speed according to

$$L_{p,\text{scaled}} = L_p(1\text{ m}) - 50\log_{10}(U/1\text{ ms}^{-1}) \tag{6}$$

The results are shown in Fig. 13. In the lower-frequency bands there is no significant difference between the Barn Owl and the Common Kestrel, but for the frequency band of 1.6 kHz and the frequency bands above, it is clear that the owl is more silent. Interestingly, the scaling made the results for the Harris Hawk and Common Kestrel very similar, at least for the higher-frequency range. These results again lead to the conclusion that the flight of the owl is quieter even when the flight speed is considered.

An additional indication for the different mechanism of sound generation found in owls is the different shape of the spectrum. For both the Common Kestrel and the Harris Hawk, the third-octave-band spectrum has a roll-off of approximately 10 dB/decade, and for the Barn Owl it is approximately 15 dB/decade. More results would be desirable to also get information about the spectral peak of the noise. However, if such a peak exists, it is obviously below or at the 500 Hz third-octave band for all tested species. Thus, the hypothesis that the sound power is simply shifted toward lower frequencies [13–15] could neither be supported nor rejected on the basis of the present results.

IV. Conclusions

Most genera of owls fly slowly and are silent to their prey when hunting. A widely accepted hypothesis is that the silent flight of the owl is not only an outcome of its low flight speed, but is also a direct consequence of its plumage adaptations that suppress flight noise generation as it is found in other bird species. Past measurements of flight noise in owls confirmed the quietness of the owl flight, but could not be used to confirm this hypothesis directly, due to the lack of comparable results from other nonsilently flying birds.

To obtain experimental results that were adequate to test this hypothesis, a study of bird flyover noise was carried out in an outdoor environment. In this study, a sophisticated setup including a 92-channel microphone array and two video cameras was developed and applied for the flyover measurements. Out of the six birds that were tested for their gliding-flight noise, three (a Common Kestrel, a Harris Hawk, and a Barn Owl) performed a number of flights that could be successfully analyzed. The results indicate that the sound pressure level for the Barn Owl is lower than that for the other two species in the frequency range above 1.6 kHz. At high frequencies above 6.3 kHz the noise from the owl is so low that it could not be measured even with the microphone array. The major noise sources for the Common Kestrel and the Harris Hawk are located at the wings, which is not the case for the Barn Owl, where the noise is produced by sources distributed over the surface of the body and wings and possibly also the feet and legs.

A scaling of the results with the fifth power of the flight speed removes the effect of different speeds of the individual flyovers. The mean values of the scaled sound pressure level of the noise made by the Barn Owl are 3 to 8 dB below the mean values of both the Common Kestrel and the Harris Hawk for all third-octave bands above 1.6 kHz. The third-octave-band spectrum in this frequency range has a roll-off of 15 dB per decade for the Barn Owl, but only 10 dB per decade for the other birds.

The different observed positions of the major sound sources with respect to the body and wings, the lower sound pressure level for higher frequencies, and the different spectral shapes of the flight noise are clear indications that the mechanism of noise generation in silently flying owls is different from that in other birds. The lower values found for the scaled sound pressure levels confirm the hypothesis that not only is the low flight speed of the owl responsible for the silent flight, but also the adaptations that distinguish the plumage of silently flying owls from that of other birds.

Acknowledgments

The authors would like to thank the staff of the wildlife park Johannismühle, especially the team of falconers who made these measurements possible. The research was sponsored as part of the priority program 1207, “Strömungsbeeinflussung in der Natur und Technik” of the *Deutsche Forschungsgemeinschaft*, under grant number SA 1502/1-2.

References

[1] Howe, M. S., “Noise Produced by a Sawtooth Trailing Edge,” *Journal of the Acoustical Society of America*, Vol. 90, No. 1, 1991, pp. 482–487. doi:10.1121/1.401273

[2] Howe, M. S., “Aerodynamic Noise of a Serrated Trailing Edge,” *Journal of Fluids and Structures*, Vol. 5, 1991, pp. 33–45. doi:10.1016/0889-9746(91)80010-B

[3] Herr, M., and Dobrzynski, W., “Experimental Investigations in Low-Noise Trailing-Edge Design,” *AIAA Journal*, Vol. 43, No. 6, 2005, pp. 1167–1175. doi:10.2514/1.11101

[4] Herr, M., “Design Criteria for Low-Noise Trailing-Edges,” *13th AIAA/CEAS Aeroacoustics Conference*, AIAA Paper 2007-3470, 2007.

[5] Geyer, T., Sarradj, E., and Fritzsche, C., “Measurement of the Noise Generation at the Trailing Edge of Porous Airfoils,” *Experiments in Fluids*, Vol. 48, No. 2, 2010, pp. 291–308. doi:10.1007/s00348-009-0739-x

[6] Geyer, T., Sarradj, E., and Fritzsche, C., “Porous Airfoils: Noise Reduction and Boundary Layer Effects,” *International Journal of Aeroacoustics*, Vol. 9, No. 6, 2010, pp. 787–820. doi:10.1260/1475-472X.9.6.787

[7] Mascha, E.,. “Über die Schwungfedern,” *Zeitschrift für Wissenschaftliche Zoologie*, Vol. 77, 1904, pp. 606–651.

[8] Graham, R. R., “The Silent Flight of Owls,” *Journal of the Royal Aeronautical Society*, Vol. 286, 1934, pp. 837–843.

[9] Sick, H., “Morphologisch-Funktionelle Untersuchungen über die Feinstruktur der Vogelfeder,” *Journal für Ornithologie*, Vol. 85, 1937, pp. 206–372. doi:10.1007/BF01905702

[10] Thorpe, W. H., and Griffin, D. R., “The Lack of Ultrasonic Components in the Flight Noise of Owls Compared with Other Birds,” *IBIS*, Vol. 104, 1962, pp. 256–257.

[11] Hertel, H., *Struktur, Form, Bewegung*, Otto Krauskopf-Verlag Mainz, Germany, 1963.

[12] Kroeger, R. A., Gruschka, H. D., and Helvey, T. C., “Low Speed Aerodynamics for Ultra-Quiet Flight,” U.S. Air Force Flight Dynamics Lab., TR 971-75, 1971.

[13] Gruschka, H. D., Borchers, I. U., and Coble, J. G., “Aerodynamic Noise Produced by a Gliding Owl,” *Nature*, Vol. 233, 1971, pp. 409–411. doi:10.1038/233409a0

[14] Neuhaus, W., Bretting, H., and Schweizer, B., “Morphologische und Funktionelle Untersuchungen Über den ‘Lautlosen’ Flug der Eulen (*Strix aluco*) im Vergleich zum Flug der Enten (*Anas platyrhynchos*),” *Biologisches Zentralblatt*, Vol. 92, 1973, pp. 495–512.

[15] Lilley, G. M., “A Study of the Silent Flight of the Owl,” AIAA Paper 1998-2340, 1998.

[16] Lilley, G. M., "The Prediction of Airframe Noise and Comparison with Experiment," *Journal of Sound and Vibration*, Vol. 239, 2001, pp. 849–859.
doi:10.1006/jsvi.2000.3219

[17] Bachmann, T., Klän, S., Baumgartner, W., Klaas, M., Schröder, W., and Wagner, H., "Morphometric Characterization of Wing Feathers of the Barn Owl *Tyto alba pratincola* and the Pigeon *Columba livia*," *Frontiers in Zoology*, Vol. 4, No. 23, 2007.
doi:10.1186/1742-9994-4-23

[18] Geyer, T., Sarradj, E., and Fritzsche, C., "Silent Owl Flight: Experiments in the Aeroacoustic Wind Tunnel," *35th Jahrestagung für Akustik (DAGA 2009)*, 2009.

[19] Guérin, S., Michel, U., Siller, H., Finke, U., and Saueressig, G., "Airbus A319 Database from Dedicated Flyover Measurements to Investigate Noise Abatement Procedure," *11th AIAA/CEAS Aeroacoustics Conference*, AIAA Paper 2005-298, 2005.

[20] Bradski, G., and Kaehler, A., *Learning OpenCV: Computer Vision with the OpenCV Library*, O'Reilly Media, Sebastopol, CA, 2008.

[21] Lucas, B. D., and Kanade, T., "An Iterative Image Registration Technique with an Application to Stereo Vision," *International Joint Conference on Artificial Intelligence*, Vol. 3, 1981, p. 3.

[22] Horn, B. K. P., and Schunck, B. G., "Determining Optical Flow," *Artificial Intelligence*, Vol. 17, Nos. 1–3, 1981, pp. 185–203.
doi:10.1016/0004-3702(81)90024-2

[23] Stoica, P., and Moses, R. L., *Introduction to Spectral Analysis*, Prentice–Hall, Upper Saddle River, NJ, 1997.

[24] Johnson, D. H., and Dudgeon, D. E., *Array Signal Processing: Concepts And Techniques*, Simon & Schuster, New York, 1992.

[25] Brooks, T. F., and Humphreys, W. M., Jr. "Effect of Directional Array Size on the Measurement of Airframe Noise Components," 5th AIAA/CEAS Aeroacoustics Conference, Bellevue, WA, AIAA Paper 1999-1958, May 1999.

[26] Sarradj, E., "A Fast Signal Subspace Approach for the Determination of Absolute Levels from Phased Microphone Array Measurements," *Journal of Sound and Vibration*, Vol. 329, 2010, pp. 1553–1569.
doi:10.1016/j.jsv.2009.11.009

[27] Sijtsma, P., and Stoker, R., "Determination of Absolute Contributions of Aircraft Noise Components Using Fly-Over Array Measurements," *10th AIAA/CEAS Aeroacoustics Conference*, Manchester, England, U.K., AIAA Paper 2004-2958, 10–12 May 2004.

[28] Brühl, S., and Röder, A., "Acoustic Noise Source Modelling Based on Microphone Array Measurements," *Journal of Sound and Vibration*, Vol. 231, No. 3, 2000, pp. 611–617.
doi:10.1006/jsvi.1999.2548

[29] Guérin, S., Weckmüller, C., and Michel, U., "Beamforming and Deconvolution for Aerodynamic Sound Sources in Motion," *1st Berlin Beamforming Conference* [CD-ROM], BeBeC Paper 2008-16, 22–23 Nov. 2006.

[30] Dougherty, R. P., "Advanced Time-Domain Beamforming Techniques," *10th AIAA/CEAS Aeroacoustics Conference*, Manchester, England, U.K., AIAA Paper 2004-2955, May 10–12, 2004.

[31] Howe, M., "A Review of the Theory of Trailing Edge Noise," *Journal of Sound and Vibration*, Vol. 61, No. 3, 1978, pp. 437–465.
doi:10.1016/0022-460X(78)90391-7

E. Gutmark
Associate Editor